J Mater Sci: Mater Med (2010) 21:847–853
DOI 10.1007/s10856-009-3888-9

Synchrotron X-ray microtomography for assessment of bone tissue scaffolds

Sheng Yue · Peter D. Lee · Gowsihan Poologasundarampillai · Zhengzhong Yao · Peter Rockett · Andrea H. Devlin · Christopher A. Mitchell · Moritz A. Konerding · Julian R. Jones

Received: 10 July 2009 / Accepted: 30 September 2009 / Published online: 10 October 2009

Abstract X-ray microtomography (μCT) is a popular tool for imaging scaffolds designed for tissue engineering applications. The ability of synchrotron μCT to monitor tissue response and changes in a bioactive glass scaffold ex vivo were assessed. It was possible to observe the morphology of the bone; soft tissue ingrowth and the calcium distribution within the scaffold. A second aim was to use two newly developed compression rigs, one designed for use inside a laboratory based μCT machine for continual monitoring of the pore structure and crack formation and another designed for use in the synchrotron facility. Both rigs allowed imaging of the failure mechanism while obtaining stress–strain data. Failure mechanisms of the bioactive glass scaffolds were found not to follow classical predictions for the failure of brittle foams. Compression strengths were found to be 4.5–6 MPa while maintaining an interconnected pore network suitable for tissue engineering applications.

1 Introduction

Natural bone healing is generally only successful if the defect is small, so when a defect exceeds ~ 1 cm^3 bone grafting is often needed. Bone tissue engineering is thought to be a promising way to regenerate lost bone where an ideal bone tissue engineering method uses a temporary template (scaffold) cultured with osteogenic cells harvested from the patient [1–3]. In this ideal scenario, the cells are expanded in culture, seeded on a scaffold in a bioreactor and once enough new tissue has been generated in vitro, the tissue/scaffold composite can then be implanted into the defect site of the patient.

The scaffold should act as both a guide and a stimulus for bone regeneration in vitro and then in vivo. The design criteria of an ideal scaffold for bone regeneration are many [1, 4]. Having a suitable interconnected porous network is important as the pore size and more importantly the interconnect size must be large enough to enable cell migration, fluid exchange and eventually bone ingrowth and vascularisation. The minimum interconnect diameter for vascularised bone ingrowth is thought to be in excess of 100 μm [5]. The mechanical properties of the scaffold should also match that of the host tissue because the scaffold needs to have enough strength to retain its structure in a load bearing environment after implantation and without being so stiff that it shields surrounding bone from load [6].

Sol–gel derived bioactive glass foam scaffolds are promising candidates for bone tissue engineering because they bond to bone, degrade in the body and release soluble silica species and calcium ions which are thought to stimulate osteogenesis at the genetic level [7–9]. In addition, the bioactive glass foam has a cancellous bone-like porous structure with suitable pore and interconnects size for tissue engineering [10].

High resolution X-ray micro-computed tomography (μCT) is a powerful tool for scaffold characterisation. Unlike many other techniques for pore and interconnect

S. Yue · P. D. Lee · G. Poologasundarampillai · Z. Yao · P. Rockett · J. R. Jones (✉)
Department of Materials, Imperial College London, London SW7 2BP, UK
e-mail: julian.r.jones@imperial.ac.uk

A. H. Devlin · C. A. Mitchell
University of Ulster, Coleraine BT52 1SA, UK

M. A. Konerding
Department of Anatomy, Johannes Gutenberg University, Mainz 55099, Germany

size quantification, including scanning electron microscopy (SEM) and mercury intrusion porosimetry (MIP), μCT can non-destructively obtain three dimensional (3D) image of a scaffold [11]. Now, when combined with 3D image analysis techniques, it can provide not only qualitative but also quantitative information of the scaffold can be obtained [10, 12].

μCT can be divided into two types in terms of X-ray sources [11]: synchrotron radiation (SR) and laboratory based Micro/Nano focus X-ray tube heads. Synchrotron μCT usually has a higher resolution, and faster scanning process than those of laboratory based μCT. Synchrotron radiation is generated from an electron storage ring and can be monochromatic (having a specific wavelength), therefore different elements can be distinguished according to their atomic number in the reconstructed images. The speed of scanning process of synchrotron μCT is massively increased compared to laboratory based μCT by the use of a finite size source (parallel) instead of point source (pencil beam).

The aim of this work was to assess whether there is a significant benefit to using synchrotron μCT over high resolution laboratory sources when characterising scaffolds for bone tissue engineering. Bioactive glass foam scaffolds are used as example scaffolds. Their pore networks were quantified using 3D image analysis and mechanical properties and failure mechanisms assessed using load cells specially designed for scanning in μCT. Tissue ingrowth and changes in scaffolds as a function of time in vivo, were also observed.

2 Materials and methods

2.1 Foam synthesis

A bioactive glass foam of the 70S30C composition (70 mol% SiO_2, 30 mol% CaO) was prepared using the sol–gel foaming method as described previously [4, 7]. The sol preparation involved mixing 0.2 mol/l nitric acid with water, followed by addition of tetraethyl orthosilicate (TEOS) and calcium nitrate (all Sigma). The molar ratio of water to TEOS (R ratio) was 12:1. Aliquots of 50 ml of the sol were foamed with vigorous agitation with the addition of 3 ml of 5 vol% HF (catalyst) and 0.35 ml of Teepol (surfactant, Thames Mead Ltd., London). As the foamed sol approached gelling point it was cast into cylindrical Teflon moulds sealed and then aged at 60°C for 72 h. The samples were then dried at 130°C, stabilised at 600°C and sintered at 800°C for 2 h.

2.2 In vivo experiment

Following general anaesthesia and surgical preparation, a cube shaped bioactive glass foam scaffold, with 1 mm dimensions, was implanted between the muscular fascia and the tibia of an 8-week-old CD1 male mouse. This study was carried out following appropriate local and national (Home Office) ethical approval. After 4 weeks, the corrosion casting of vessels was performed as detailed previously [13] by trans-cardiac perfusion with Mercox CL-2B (Vilene Med Co, Tokyo Japan) diluted with 20% methylmethacrylate monomers (Merck Darmstadt, Germany). Upon complete polymerization, the entire lower limbs containing the scaffolds were removed, fixed in 10% neutral buffered formalin and the surrounding tissue dissected free to allow easy placement of the sample in the chamber. The samples were imaged using monochromatic synchrotron μCT (ESRF, Grenoble, France; Beamline ID19) with a special resolution of 0.55 μm. The reconstructed image was then rendered with commercial image analysis packages (VGStudio MAX 1.2, Volume Graphics GmbH, Heidelberg, Germany).

2.3 3D image analysis and compression testing

Interrupted compression test was performed on a bioactive glass foam specimen (width 1.08 mm, depth 1.08 mm, height 2.3 mm). The scaffold was scanned at each step with synchrotron μCT (ESRF, Grenoble, France; Beamline ID19) using a selected beam energy of 20 keV using the multilayer monochromator available at the beam line with a 1.4 μm resolution. Images were reconstructed using a parallel-beam filtered back-projection algorithm (ESRF, Grenoble, France). A schematic of the load cell is shown in Fig. 1a, which was developed by the ESRF team. Before samples were compression tested, their pore structure was imaged and quantified as described below. The load was then applied to the sample using the screw thread that was attached to the upper platen, after which was then re-scanned. Quarter turns of the thread were applied between each scan, which corresponded to load steps of 0.3–0.7 N. These steps were repeated until the sample failed. Importantly, the images from the interrupted compression test were registered by an ITK based routine [14] so that the images taken from each step were aligned by the non-deformed part of the bioactive glass foam in the images.

The pore and interconnect sizes of the scaffold were quantified with algorithms which have been described previously [10, 12], including a dilation based distance transform, a 3D watershed algorithm [14, 15], and a novel in house algorithm to locate the interconnects. [10, 12]. The size of the spherical pore was represented by the diameter length of a sphere with equivalent volume. The quantification of the interconnect size has been improved by a principle component analysis (PCA) based method. The PCA based method can find the natural moment of the interconnects by calculating the eigensystem of the

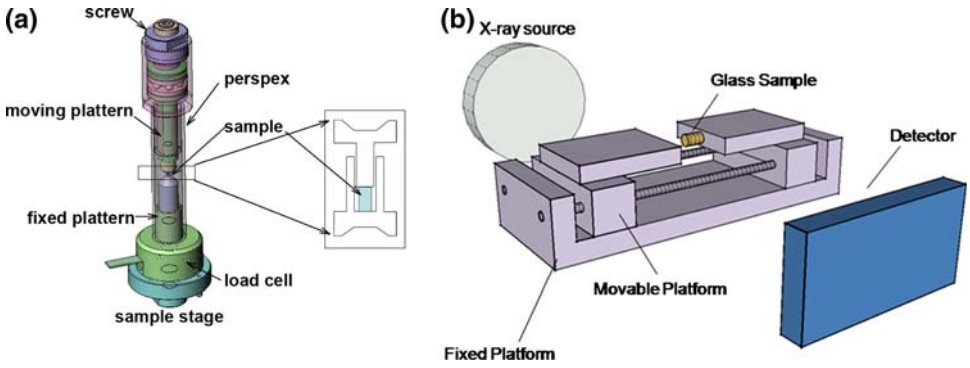

Fig. 1 Schematics of the compression rigs used in the μCT machines, **a** rig used with synchrotron μCT (ESRF), and **b** rig used for in situ testing in a laboratory μCT

covariance matrix of its voxels coordinates in the image. Then the interconnect voxels can be projected to its principle plane and the area of the interconnect can be calculated by a convex hull algorithm.

2.4 In situ compression

Using an in-house developed compression rig (Fig. 1b), the compressive strength of similar scaffolds was assessed while they were in the X-ray beam of a laboratory based μCT machine. Scaffolds with sintering temperatures of 600°C and 800°C were compared. Seven samples (3 mm × 3 mm × 5 mm) of each were tested. The rig's main components included a Harmonic drive ME-02-L rotary encoder, a Heidenhain 602E linear encoder, a Harmonic drive RH-8-3006 actuator, an ENTRAN ELFS-T3M-250N load cell, a stationary platen and a mobile platen. The rotary encoder was the driver for the moving platen while the calibrated linear encoder (0.1 μm resolution) read the displacement of the platform. The load cell was 250 N but the maximum load applied during testing was restricted to below 180 N. The shafts are isolated with air-bearings to provide sufficient lubrication to protect the system from any static and dynamic frictional forces. A NextMove NBA-100-MC01 control board was used to provide communication between the testing system and the accompanying WorkBench software in a Windows operation system. This rig enabled 2D transmission images of the scaffold to be captured in real time under continual strain, while load/compression data was collected at a strain rate of 0.001 mm s^{-1}. Transmission images were collected every 0.4 s. Mode of failure and crack path could therefore be observed.

3 Results and discussion

3.1 Synchrotron imaging of explanted scaffolds and tissue

Figure 2a shows a synchrotron μCT image of a bioactive glass scaffold. Figure 2b shows μCT images of a similar scaffold and surrounding tissue ex vivo, following 4 weeks implantation between the muscle and tibia of a mouse. The images are child volumes of the explant, enabling visualisation of important features. The tubular tibia is clearly imaged, with the resolution high enough to visualise the lacunae within the bone (Fig. 2b zoom). At the level at which the cross-section in Fig. 2b is taken, the mouse bone has lower density at the outside compared to the bone closer

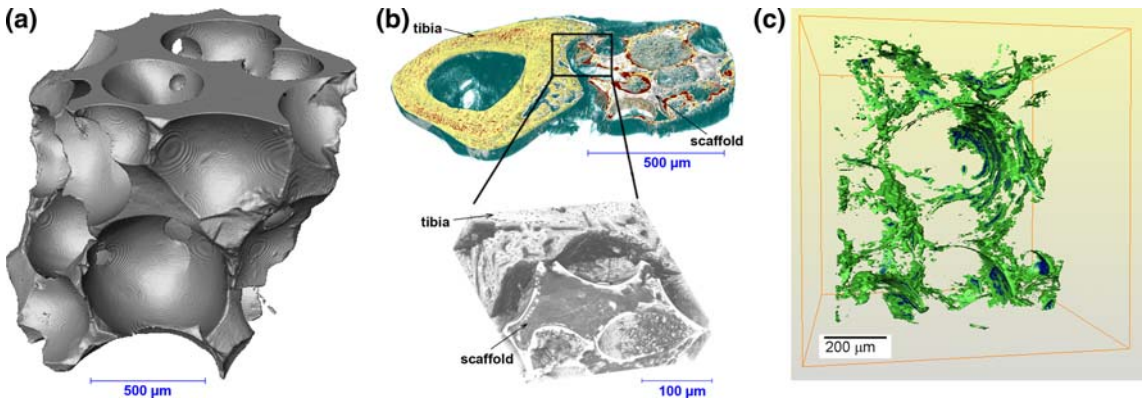

Fig. 2 Synchroton μCT images of **a** a bioactive glass scaffold, **b** a scaffold next to a mouse tibia ex vivo after 4 weeks implantation (child volumes)

to the marrow cavity (also observed in the control of a scan of a tibia without a scaffold implanted). The corrosion casting enables visualisation of blood vessels and soft tissue around the scaffold and inside the pores. Figure 2b shows some tissue growing into the pores of the scaffold, however it is not possible to identify the tissue type using this technique. Although specific tissue type cannot be identified, μCT gives qualitative information on the density of the tissue and material. The tissue growing into the pore is of lower density than the scaffold, indicating that it is soft tissue, such as fibro-collagenous matrix. This matrix is most likely fibrous tissue forming as a result of micromotion between the scaffold and the tibia, which is likely as the scaffold was not implanted into a bone defect or secured with any fixation methods. Importantly, Fig. 2b shows that changes in the scaffold can be observed with implantation time, for example, bright regions can be observed within the scaffold struts and around the walls of some of the pores (marked in red and bright regions in the zoomed image). This corresponded to calcium rich regions, which result from dissolution of calcium from the glass, leaving some areas calcium rich, and reprecipitation of the calcium on the scaffold surface after dissolution. Some of the calcium rich regions were more dense than the mouse bone and they were identified as being calcium carbonate (XRD, data not shown). Calcium carbonate is thought to form in regions of low flow rate. Other calcium rich regions were of similar density to the bone mineral, which could have been apatite rich. Figure 2c shows an image representing the calcium distribution within an as-prepared bioactive glass foam scaffold, obtained using the synchrotron μCT, with the image of the scaffold itself removed. Such images are not possible to obtain with laboratory based μCT. The calcium distribution follows the contours of the macropores and is higher in concentration near the surface, which is due to the synthesis method. The calcium source in the sol–gel process is calcium nitrate, which has recently been found to leave the gel during gelation, precipitate onto the surface of the gel during drying with the calcium only migrating into the silica network as the temperature rises above 350°C [16]. Figure 2 illustrates the level of detail that can be achieved with synchrotron μCT. The images in Fig. 2b could be compared to histological slices to verify tissue type. Laboratory based μCT cannot produce images of such high quality that can be compared directly to histological slices.

3.2 Bioactive glass foam failure mechanisms

Synchrotron μCT was used to image samples as a function of compressive load. This was an interrupted test as scans were carried out after each time the load was increased in order to obtain 3D images. The load cell in Fig. 1a was designed especially for such experiments. The great advantage of using this device was that it could remain in the beam line so that it was easy to register the images obtained to those obtained in previous scans, so that changes in specific pores could be observed and quantified. Figure 3a shows a 3D reconstructed μCT image of the scaffold that was tested. Before testing, the pore network was quantified using 3D image analysis techniques. Figure 3b shows the pores within the scaffold, obtained by thresholding, using the dilation algorithm to create a distance map, to which a watershed algorithm to applied to identify the pores. The PCA method was then used to identify and quantify the interconnects. The results of the image analysis are shown in Fig. 4, with a few of the individual pores/interconnects dimensioned in Fig. 3b. Figure 3c shows the same scaffold after it was loaded until total rupture at failure at 7 N, corresponding to a stress of 6 MPa. Little difference could be observed in the 3D images of the foam until this point. The load displacement curve showed that failure occurred at 5.2 N, which corresponds to a σ_{max} of approximately 4.5 MPa, which was similar to the compressive strength obtained from larger similar scaffolds (cylinders 29 mm diameter, 9 mm height) tested with conventional Instron [4]. The advantage of μCT is that the user can virtually pass through the sample slice by slice, which can allow identification of cracks. As shown in Fig. 3d (preload was 2 N) and e (load was 5.2 N), smaller volumes were extracted from Fig. 3a and c respectively. Figure 3e shows nucleation of a crack at a load 5.2 N. This volume was taken from the volume close to the moving platen, which was at the top of Fig. 3a.

Returning to the 3D image analysis of the scaffold prior to testing (Fig. 4), the results show that the pore network was suitable for tissue engineering applications with a mean pore size of 265 μm and a mean interconnect size greater than 100 μm. Figure 4a shows that the majority of pores were in the range 100–300 μm and Fig. 4b shows that 17 of the 20 interconnects had diameters in the range 50–200 μm and half the total interconnects were in excess of 100 μm in diameter. During time of implantation the interconnect size is expected to increase as dissolution occurs.

Compression testing was also carried out in situ, using a bespoke compression tester (Fig. 1b) inside a laboratory μCT machine, using real time radiography to track crack growth. Figure 5a shows a transmission image of the scaffold under a 2 N preload prior to testing. Figure 5b–e show successive transmission images of the scaffold under increasing strain. The highlighted regions in Fig. 5b show the initiation of a crack at a strain of 0.006 (stress of 2.4 MPa), which then progressed through the sample (Fig. 5c). As strain increased to 0.008 (stress of 3.2 MPa), further cracks nucleated (arrows in Fig. 5c). Figure 5d shows that the crack ran through the entire scaffold when the strain reached 0.015 (stress of 6.2 MPa), and then

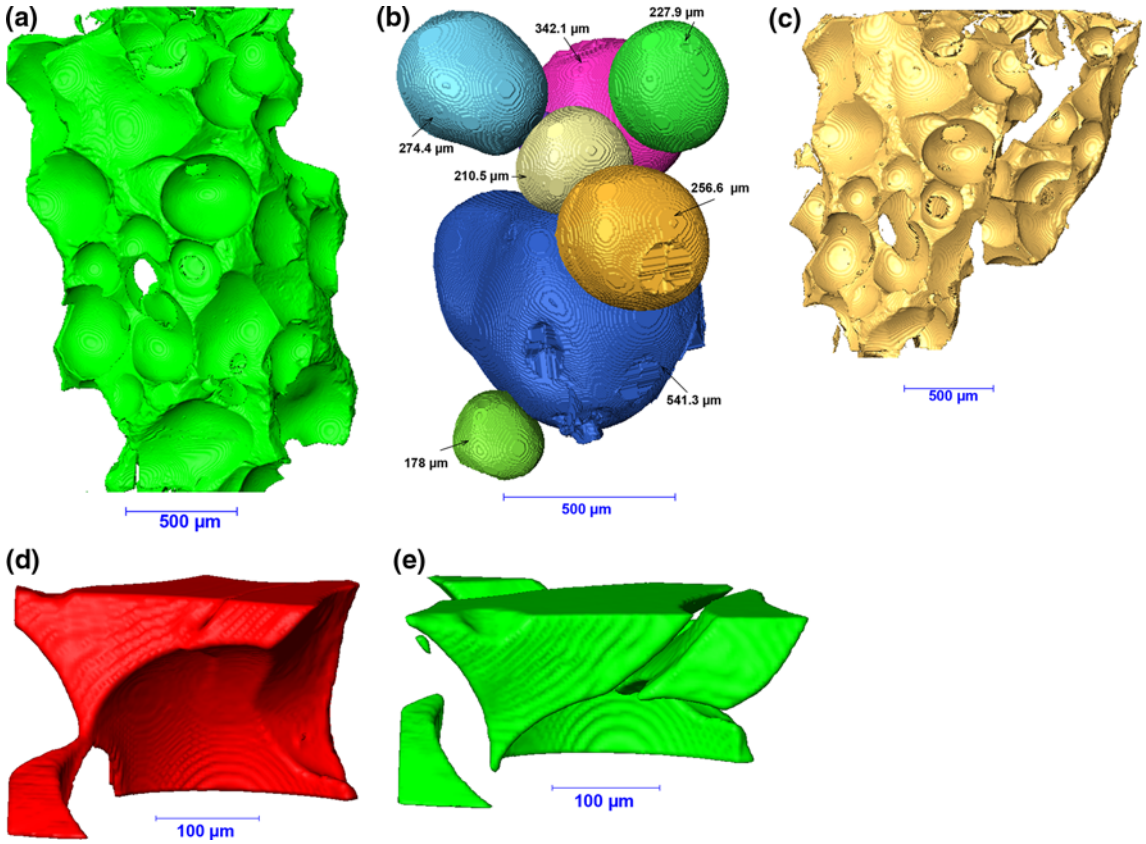

Fig. 3 **a** Synchroton µCT image of a scaffold in the compression rig shown in Fig. 1a, **b** pores within the scaffold in **a**, identified by image analysis algorithms, **c** synchroton µCT image of the same scaffold after failure in compression, **d** child volume of a section of the scaffold under 2 N load, prior to failure, and **e** the same child volume after crack initiation

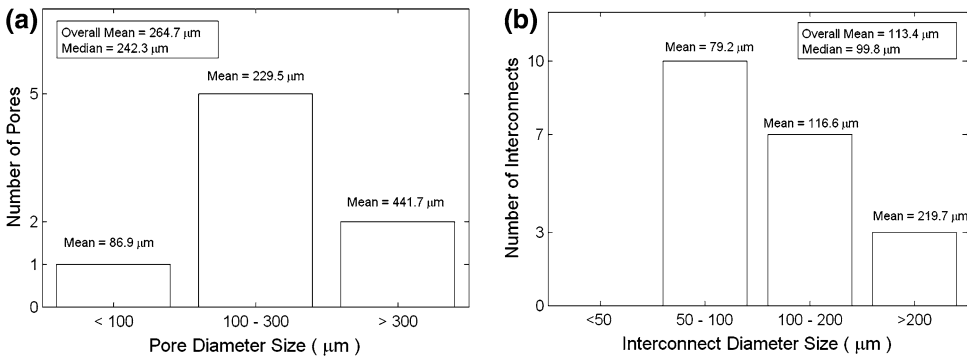

Fig. 4 Quantification of the pore network of the bioactive glass foam scaffold prior to compression testing in the synchrotron µCT using 3D image analysis algorithms **a** pore diameter, and **b** interconnect diameter

larger sections of the scaffold began to rupture and be displaced, e.g. the tope right hand region of the scaffold in Fig. 5d. According to Gibson and Ashby [17], brittle porous foams with interconnected pores should fail one pore layer at a time, through rupture of the struts in one pore layer, which results in the collapse of that layer. Crack propagation would therefore be perpendicular to the load direction. As strain continues, the struts in the next layer of pores will rupture and so on. However, in the scaffolds tested here, the crack propagated parallel to the load direction. This could be due to the random, rather than regular, pores arrangement within these scaffolds (the Gibson and Ashby model was based on a regular honeycomb morphology). Fracture appears to initiate a single pore distance away from a platen, where a strut that stands proud at the rough edges of the scaffold is forced down into the next pore layer. At the triple point junction with the next pore, a strong bending moment is initiated and a strut wall ruptures, with the crack propagating quickly along it. This in turn propagated down another layer as the crack widens, nucleating further cracks. The images also show that the elastic deformation was not homogeneous. The

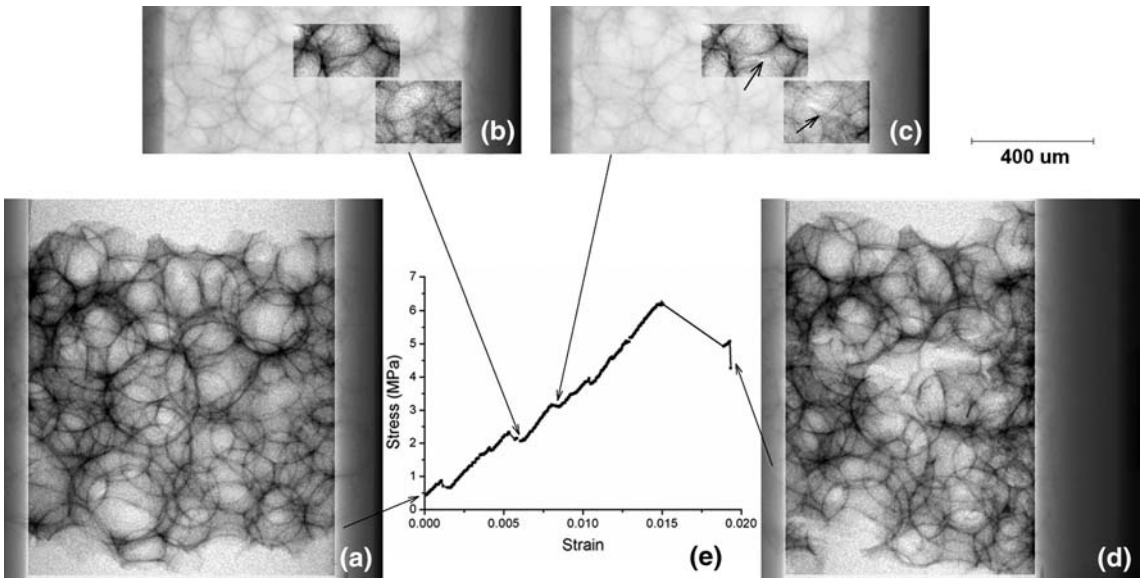

Fig. 5 **a–d** Transmission μCT images of a bioactive glass scaffold undergoing compression during in situ compression testing inside a laboratory based μCT machine and **e** the stress–strain curve obtained

right side of the scaffold, which was adjacent to the moving platen, underwent more deformation than the rest of the scaffold. Figure 5e shows a typical stress strain curve for a glass scaffold in the in situ compression rig. The steps in the curve correspond to rupture of pore walls and crack progression. This work demonstrates that it is possible to monitor crack nucleation and progression while collecting a stress–strain curve for porous scaffolds, using a testing rig designed for use in a high resolution laboratory based μCT machine.

4 Conclusions

Synchrotron μCT can be used to obtain high resolution images of explanted scaffolds and bone tissue. Resolution of mouse explants is sufficient to identify porosity and morphology of the bone and mineral distribution within the scaffold pores and struts. Using the corrosion casting technique on sacrifice of the mouse allows imaging of microvessel development around and inside the scaffold. There is a clear benefit of using the synchrotron over laboratory based μCT.

Compression testing in especially designed rigs that can fit inside the μCT machines combined with image analysis techniques allow simultaneous quantification of the pore structure, imaging of crack initiation, determination of crack path and mode of failure while obtaining compression strength data.

Acknowledgements Julian Jones is a Royal Academy of Engineering/Engineering and Physical Science Research Council (EPSRC) Research Fellow. The authors also acknowledge financial support from the Philip Leverhulme Prize and EPSRC (GR/T26344). The European Synchrotron Radiation Facility especially the team of beam line ID19, especially Elodie Boller is greatly acknowledged for the provision of synchrotron radiation facilities.

References

1. Langer R, Vacanti JP. Tissue engineering. Science. 1993;260:920–6.
2. Takezawa T. A strategy for the development of tissue engineering scaffolds that regulate cell behavior. Biomaterials. 2003;24:2267–75.
3. Ohgushi H, Caplan AI. Stem cell technology and bioceramics: from cell to gene engineering. J Biomed Mater Res. 1999;48:913–27.
4. Jones JR, Ehrenfried LM, Hench LL. Optimising bioactive glass scaffolds for bone tissue engineering. Biomaterials. 2006;27:964–73.
5. Hulbert SF, Morrison SJ, Klawitte JJ. Tissue reaction to three ceramics of porous and non-porous structures. J Biomed Mater Res. 1972;6:347–74.
6. Yang S, Leong KF, Du Z, Chua CK. The design of scaffolds for use in tissue engineering. Part I. Traditional factors. Tissue Eng. 2001;7:679–89.
7. Sepulveda P, Jones JR, Hench LL. Bioactive sol–gel foams for tissue repair. J Biomed Mater Res. 2002;59:340–8.
8. Xynos ID, Edgar AJ, Buttery LDK, Hench LL, Polak JM. Gene-expression profiling of human osteoblasts following treatment with the ionic products of Bioglass (R) 45S5 dissolution. J Biomed Mater Res. 2001;55:151–7.
9. Hench LL, Polak JM. Third-generation biomedical materials. Science. 2002;295:1014–7.
10. Jones JR, Poologasundarampillai G, Atwood RC, Bernard D, Lee PD. Non-destructive quantitative 3D analysis for the optimisation of tissue scaffolds. Biomaterials. 2007;28:1404–13.
11. Stock SR. X-ray microtomography of materials. Int Mater Rev. 1999;44:141–64.

12. Atwood RC, Jones JR, Lee PD, Hench LL. Analysis of pore interconnectivity in bioactive glass foams using X-ray microtomography. Scripta Mater. 2004;51:1029–33.
13. Konerding MA. Scanning electron-microscopy of corrosion casting in medicine. Scanning Microsc. 1991;5:851–65.
14. Ibanez L, Schroeder W, Ng L, Cates J. The ITK software guide. Clifton Park, NY: Kitware Inc.; 2003.
15. Mangan AP, Whitaker RT. Partitioning 3D surface meshes using watershed segmentation. IEEE Trans Vis Comp Graph. 1999;5: 308–21.
16. Lin S, Ionescu C, Pike KJ, Smith ME, Jones JR. Nanostructure evolution and calcium distribution in sol–gel derived bioactive glass. J Mater Chem. 2009;19:1276–82.
17. Gibson LJ, Ashby MF. Cellular solids structure and properties. Oxford: Pergamon Press; 1988.